Electronic Supplementary Material (ESI) for Nanoscale Horizons.

Electronic Supplementary Information: Growth Mechanisms from Tetrahedral Seeds to Multiply Twinned Au Nanoparticles Revealed by Atomic Level Simulations

El yakout El koraychy,[a] Cesare Roncaglia,[a] Diana Nelli,[a] Manuella Cerbelaud,[b] and Riccardo Ferrando[c]

[a] *Dipartimento di Fisica dell'Università di Genova, via Dodecaneso 33, Genova 16146, Italy*
[b] *Université de Limoges, CNRS, IRCER, UMR 7315, F-87000 Limoges, France*
[c] *Dipartimento di Fisica dell'Università di Genova and CNR-IMEM, via Dodecaneso 33, Genova 16146, Italy*

Contents

1 Gupta force field and growth simulation method **3**

2 Gupta and DFT data on adsorption energies on tetrahedra **4**

3 Supplementary growth simulations results **6**

1 Gupta force field and growth simulation method

The atomistic potential has the form proposed by Gupta [4] and by Rosato *et al.* [10]. This force field can be derived from the second moment approximation to the tight-binding model [2]. The potential energy E is given the sum of atomic contributions E_j, $j = 1, ..., N$ where N is the number of atoms. E_j is given by

$$E_j = \sum_i A \exp\left[-p\left(\frac{r_{ij}}{r_0} - 1\right)\right] - \sqrt{\sum_i \xi^2 \exp\left[-2q\left(\frac{r_{ij}}{r_0} - 1\right)\right]}, \quad (1)$$

where r_{ij} is the distance between atoms i and j, r_0 is the nearest-neighbor distance in the Au bulk lattice. Cutoff distances on the interactions are imposed as follows. The exponentials in Eq. (S1) are replaced by fifth-order polynomials, of the form $a_3(r - r_{c2})^3 + a_4(r - r_{c2})^4 + a_5(r - r_{c2})^5$, between distances r_{c1} and r_{c2}, with a_3, a_4, a_5 fitted to obtain continuous functions, with first and second derivative for all distances. The polynomial must tend to zero at r_{c2}.

The parameters of the potential (see Table S1) were taken from Ref. [1], where they have been favourably tested against DFT calculations.

p	q	A (eV)	ξ (eV)	r_0 (Å)	r_{c1} (Å)	r_{c2} (Å)
10.5300	4.3000	0.2197	1.8550	2.87792	4.07000	4.98471

Table S 1: Parameters of the Gupta potential for Au. From Ref. [1].

Molecular Dynamics (MD) were made by means of the same method as in Refs. [11, 12], using our own MD codes. Simulations start from a tetrahedral seeds on which Au atoms are deposited one by one from random directions in an isotropic way. Atoms are deposited at a constant rate. Rates used in the simulations are in the range from 0.1 to 10 atoms/ns. The equations of motion are solved by the Velocity Verlet algorithm with a time step of 5 fs. Temperature is kept constant by an Andersen thermostat. The simulations at faster deposition rates and for relatively small sizes are run by the CPU version of the code, whereas simulations for larger sizes are run by the GPU version.

2 Gupta and DFT data on adsorption energies on tetrahedra

In Table S2 we report the adsorption energies of Au adatoms on a tetrahedron of 84 atoms (i.e. for total size of the cluster of 85 atoms). The positions of the adsorption sites are shown in Figure S1. The adsorption energies were calculated by the Gupta force field and by Density Functional Theory (DFT), using three different exchange-correlation functional: Perdew-Burke-Ernzerhof (PBE) [8] functional, a revised version of PBE which improves the description of bulk solids (PBEsol) [9] and the Local Density Approximation (LDA) [7]. The zero of the energy is the most favorable adsorption site, which turns out to be the hcp edge site in all cases. All DFT calculations show that the adsorption in the vicinity of the edge is considerably much more favorable than in internal sites, confirming the Gupta results. This preferential adsorption effect is even stronger according to DFT than according to Gupta.

All DFT calculations were made with the open-source QUANTUM ESPRESSO software [3]. For all functionals, the convergence thresholds for the total energy, total force, and for electronic calculations were set to 10^{-4} Ry, 10^{-3} Ry/au and $5 \cdot 10^{-6}$ Ry respectively. The size for the cubic cell side was set to 30 Å, with the only exception for the PBEsol functional, for which instead 25 Å were used. These conditions ensured that minimum distances between adjacent periodic images in each direction were at least 10 Å. Cutoffs for wavefunction and charge density were set to 26 and 435 Ry, 41 and 364 Ry, 26 and 650 Ry for LDA, PBE and PBEsol respectively, according to Au.pz-dn-kjpaw_psl.0.1.UPF, Au.pbe-n-kjpaw_psl.1.0.0.UPF and Au.pbesol-dn-kjpaw_psl.0.1.UPF, as provided by the QUANTUM ESPRESSO pseudopotential library currently available at `https://pseudopotentials.quantum-espresso.org/legacy_tables/ps-library/au`.

	Gupta	PBE	PBEsol	LDA
(a) hcp edge	0.000	0.000	0.000	0.000
(b) fcc edge	0.045	0.128	0.134	0.138
(c) hcp terrace	0.111	0.159	0.160	0.168
(d) fcc terrace	0.116	0.196	0.183	0.184

Table S 2: Energies (in eV) of an Au adatom on the surface of an Au tetrahedron of 84 atoms according to the Gupta potential and to DFT calculations with different exchange-correlation functionals. (a-d) refer to the adsorption sites of Figure S1. The adsorption energy in site (a) is set to zero.

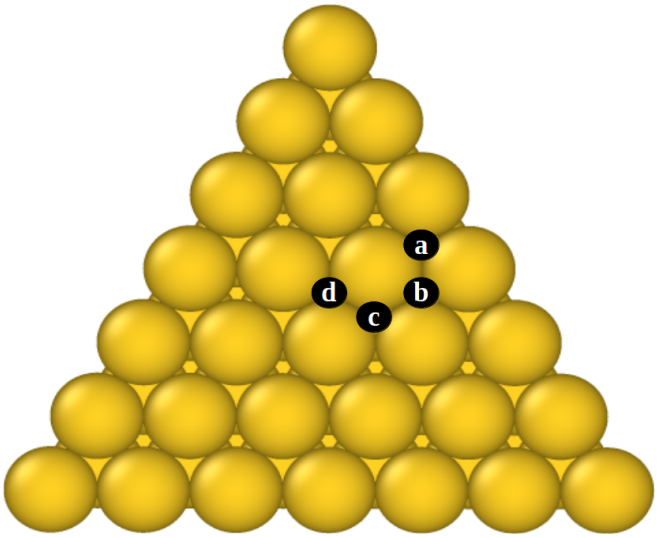

Figure S 1: Adsorption sites on the face of an Au tetrahedron of 84 atoms. (a) hcp site at the facet edge; (b) fcc site at the facet edge; (c) hcp site on the terrace; (d) fcc site on the terrace.

3 Supplementary growth simulations results

In Figure S2 the formation of a fivefold axis in a simulation at $T = 300$ K and deposition rate $r_{dep} = 1$ atom/ns is shown. The simulation starts from a perfect tetrahedron of 220 atoms.

In Figure S3 we report snapshots from a simulation at $T = 500$ K and $r_{dep} = 1$ atom/ns in which the Th→Dh growth process is shown.

Figure S4 shows the direct evolution from a tetrahedron to an icosahedral fragment, i.e. a Th→Ih process.

Figure S5 shows the growth of a double tetrahedron, i.e. the Th→dTh process.

In Figures S6 and S7 we show the evolution of 10 independent simulations at r_{dep}= 1 and 10 atoms/ns, respectively. Simulation temperature is $T = 500$ K. All simulations start from a slightly truncated tetrahedron of 356 atoms.

In Figures S8-S11 we report simulations of the growth on top of Ag and Pd tetrahedra, which show that the qualitative behaviour of these systems is the same as in Au. First, we observe an initial stage in which the sharp tips of the tetrahedron become slightly truncated. Then the growth continues by the formation of islands in stacking fault that, once stabilized, trigger the nucleation of one or more fivefold axes. In Figure S10 the simulation starts from a tetrahedron with a deeper truncation of one of the tips, but the following growth steps are hardly influenced by this different initial condition. In these simulations, the Gupta potential is used, with potential parameters taken from Ref. [5] for Ag and [6] for Pd.

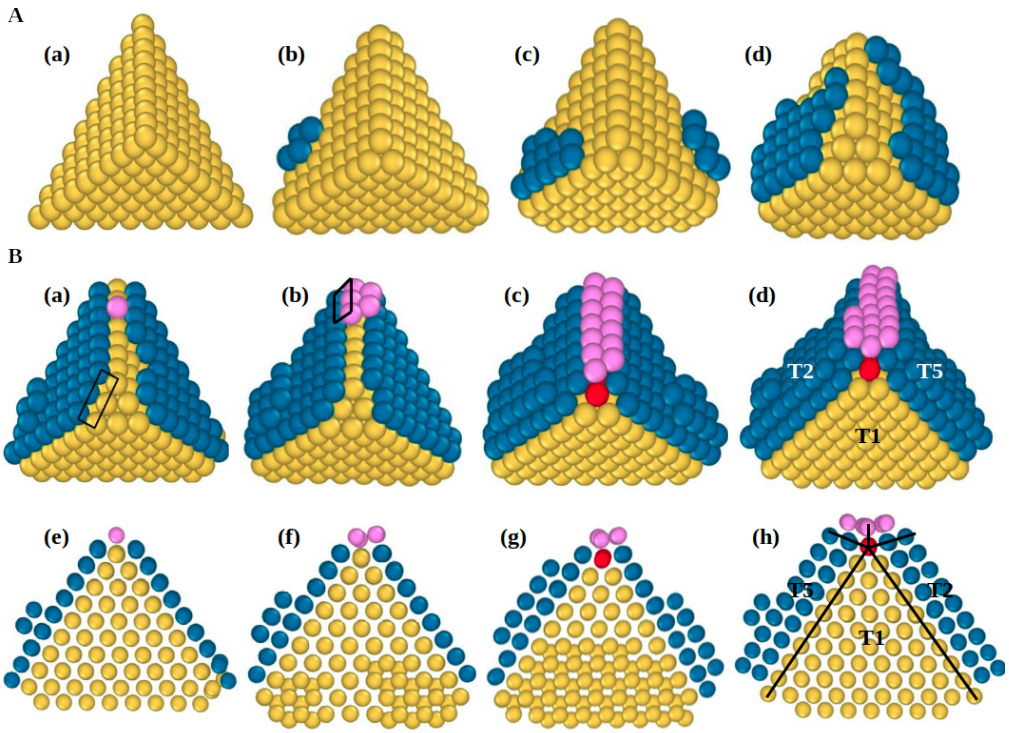

Figure S 2: Emergence of fivefold axis on a tetrahedral seed during the growth of a decahedral Au nanoparticle. Snapshots are taken for a growth simulation at $T = 300$ K and $r_{dep} = 1$ atom/ns started from a perfect tetrahedron of 220 atoms. The figure is divided into part A (first row) and part B (second and third row). – A) Tetrahedron symmetry breaking. (b) Truncation of vertices and migration of apex atoms to the nearby facets to form an hcp faulted islands. c) A second faulted island is formed on a neighboring facet. (d) Growth of the two faulted islands (blue atoms) on two different facets over four. – B) Emergence of a fivefold axis and development of twin planes on two adjacent (111) facets of the initial tetrahedron. The black rectangles enclose the fourfold adsorption sites. (a) A valley between two adjacent tetrahedral facets with faulted layers is formed. (b) An atomic row (pink atoms) in the valley starts to grow in order to connect the two faulted facets of tetrahedron creating fourfold sites, on which (c)-(d) new atoms (pink atoms) adsorb leading to the appearance of the fivefold axis. Atoms of the fivefold axis are colored in red. (e), (f), (g) and (h) show the same structures of (a), (b), (c) and (d) from another orientation. The straight black lines in (h) mark the twin boundaries of the decahedral fragment.

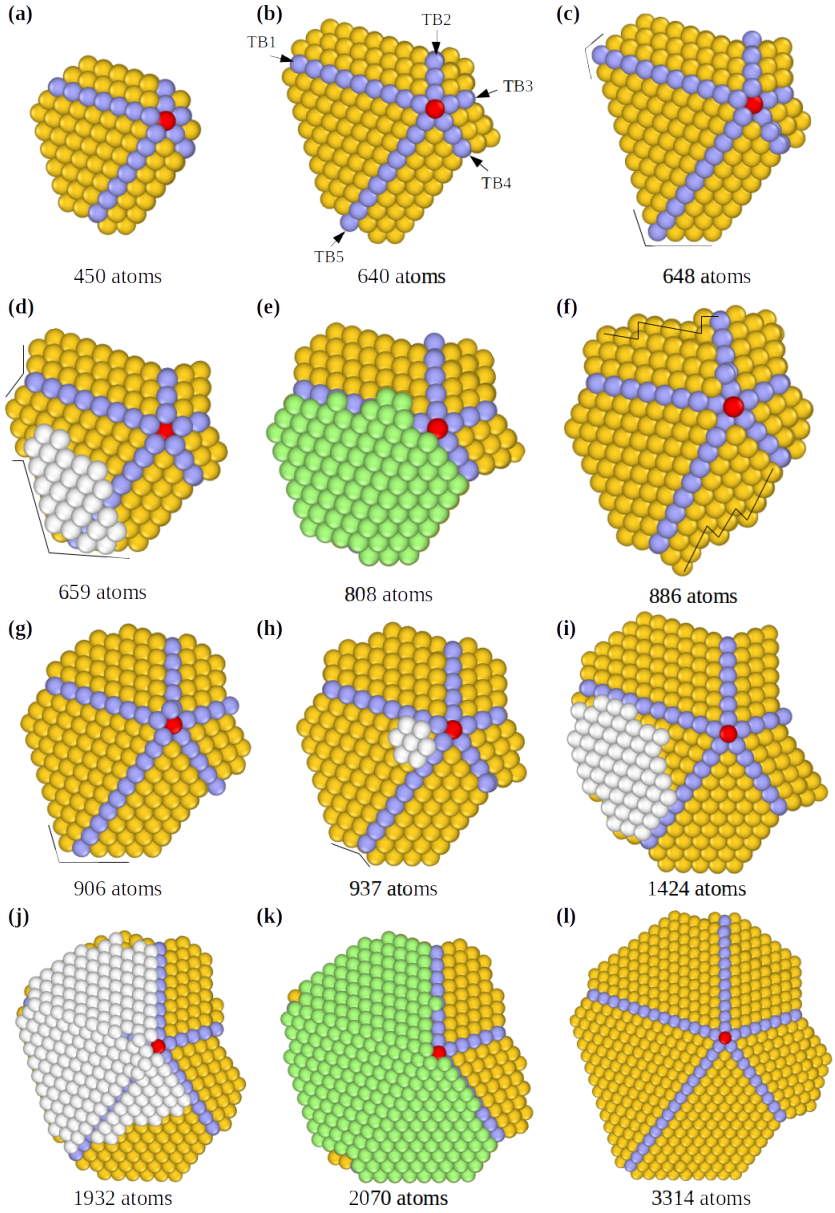

Figure S 3: Snapshots from a simulation of decahedral growth at $T = 500$ K and $r_{dep} = 1$ atom/ns. Atoms colored in violet correspond to the twin boundaries between tetrahedral units, red atoms show the fivefold axis. Atoms of capping islands hcp stacking are shown in white, but they become green when the islands revert to fcc stacking. The black arrows indicate the five twin boundaries. (a) Initial stage of the formation of the fivefold axis and of the five twin boundaries (TB1 – TB5) and of the five tetrahedra (b). (c) and (d) show the disappearance of the sharp decahedral tips to a form reentrant grooves by migration of their atoms to the nearest (111) facet of the initial tetrahedron where they form a faulted island. (e) This island reverts back to fcc stacking and (f) completes a further capping layer on the decahedron. This process is repeated at a later stage, as shown in (g)-(l).

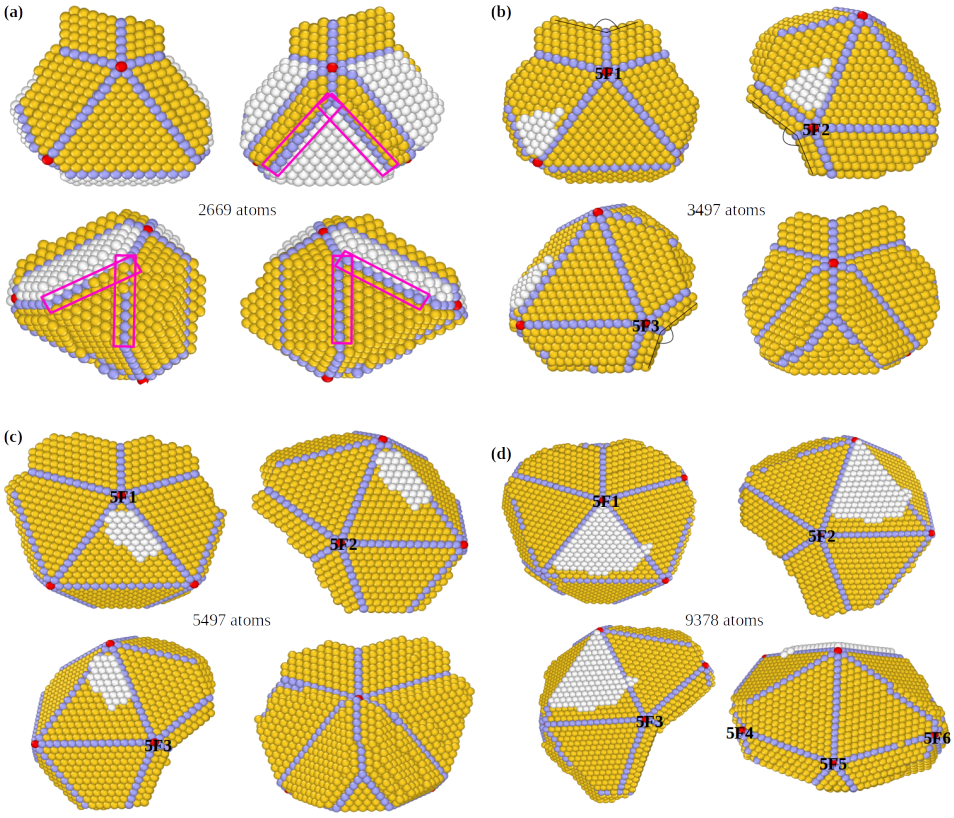

Figure S 4: Growth of an icosahedral fragment at $T = 500$ K and $r_{dep} = 1$ atoms/ns. For each size, the structure is shown from four different perspectives. (a) Structure after the stabilization of three faulted islands on the (111) facets of the initial tetrahedral seed which leads to the emergence of three fivefold axes (red atoms). The purple rectangles enclose the fourfold adsorption sites close to two twin boundaries which trigger the growth of other tetrahedral sub-units (b). (c) Four almost complete tetrahedra are formed simultaneously and in conjunction with six truncated tetrahedra. (d) Three new fivefold axes are established.

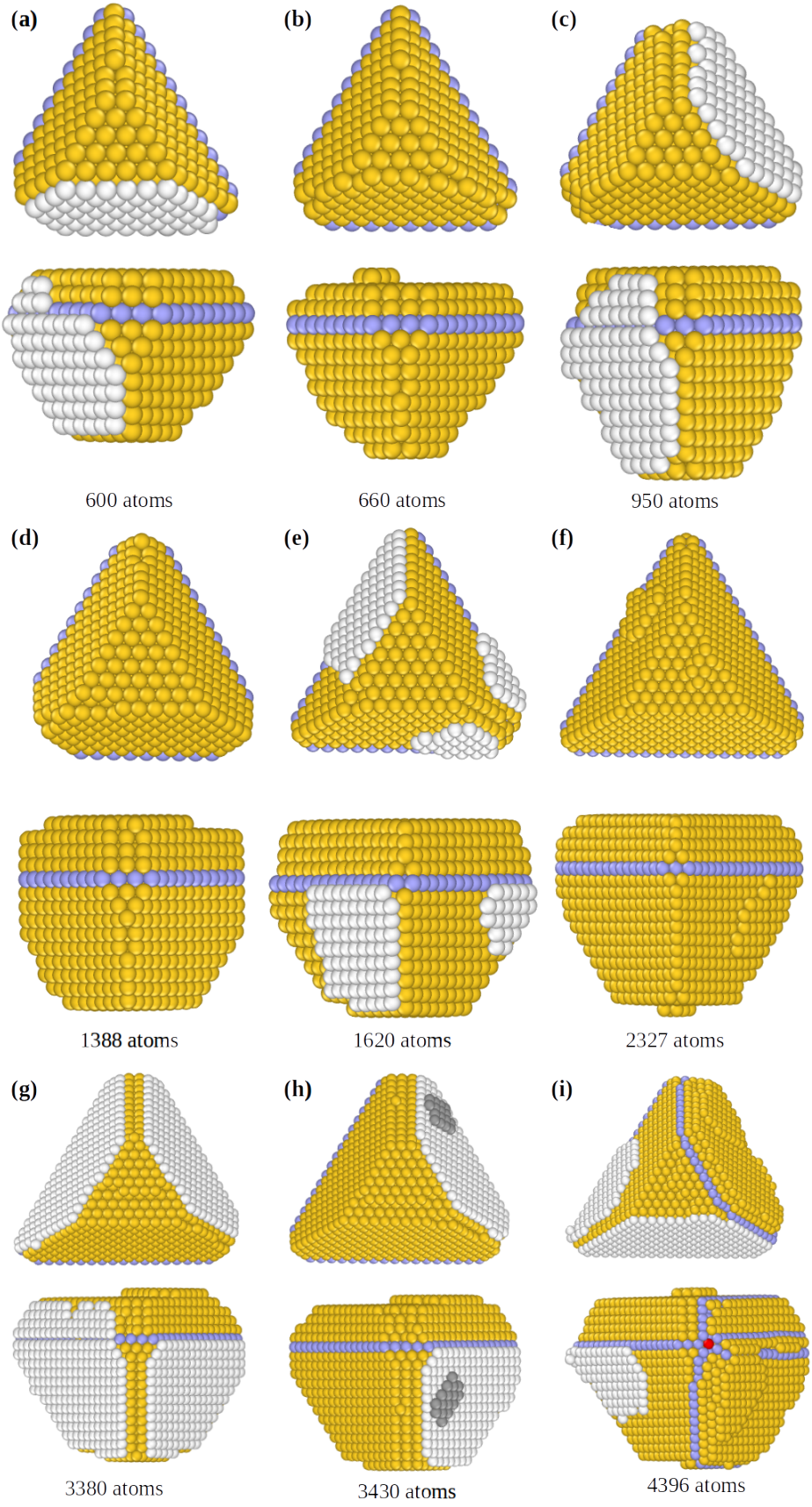

Figure S 5: Growth of truncated bi-tetrahedral units at 500 K and flux of 1 atoms/ns. For each size, the image is taken from two different perspectives. Islands in hcp stacking often form (shown by the atoms in white) but they revert back to the fcc stacking as growth continues.

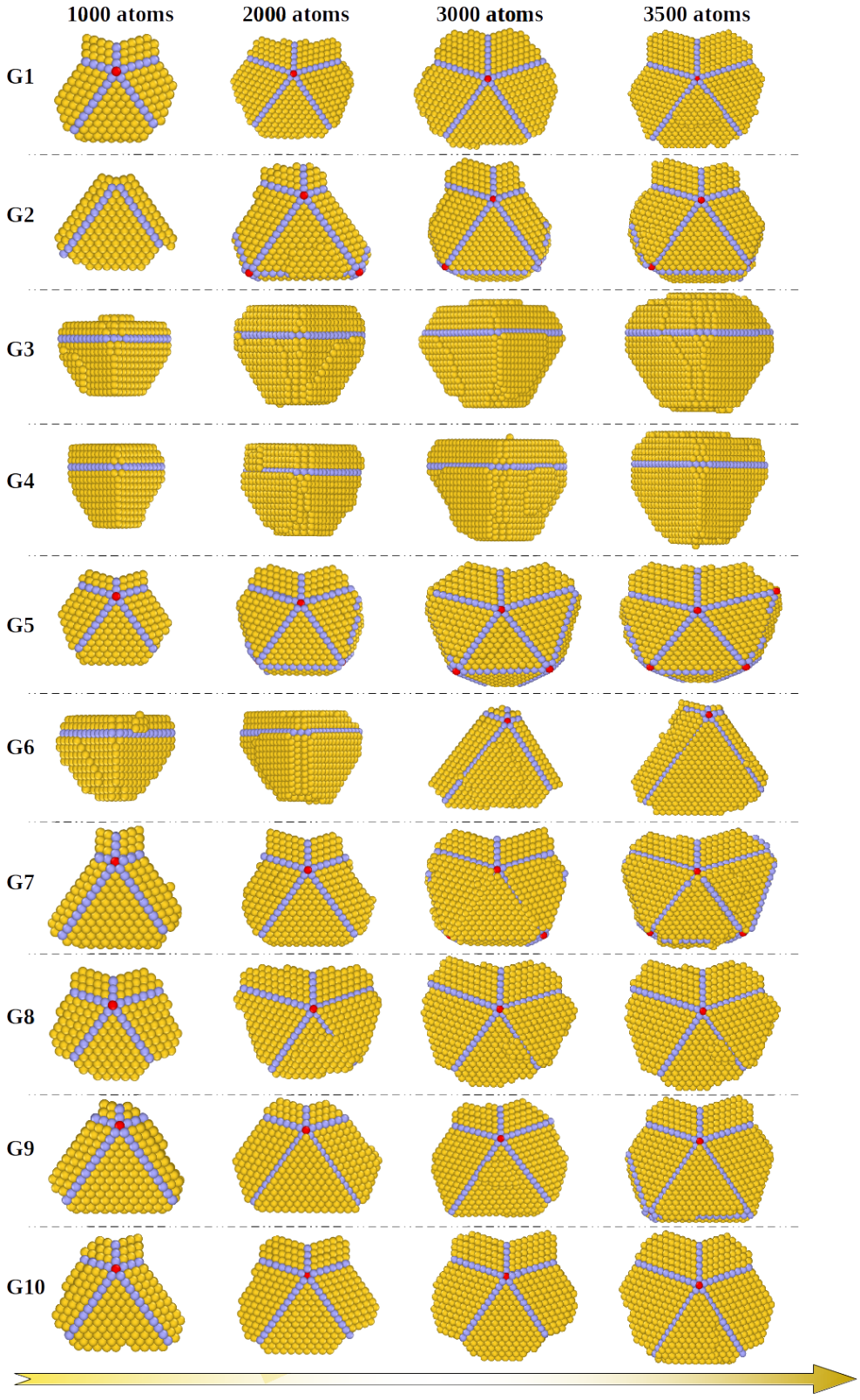

Figure S 6: Structures of 10 molecular dynamics simulations at different sizes for temperature 500 K and deposition rate of 1 atom/ns. Simulations start from a tetrahedral structure of 356 atom. In each simulation (each row), the four snapshots are taken at sizes 1000, 2000, 3000 and 3500 atoms from left to right. At 1000 atoms, we obtain 6 truncated Dh and 4 truncated Th with twin plane. At 3500 atoms, there are 4 Dh structures, 2 dTh and 2 Ih fragments.

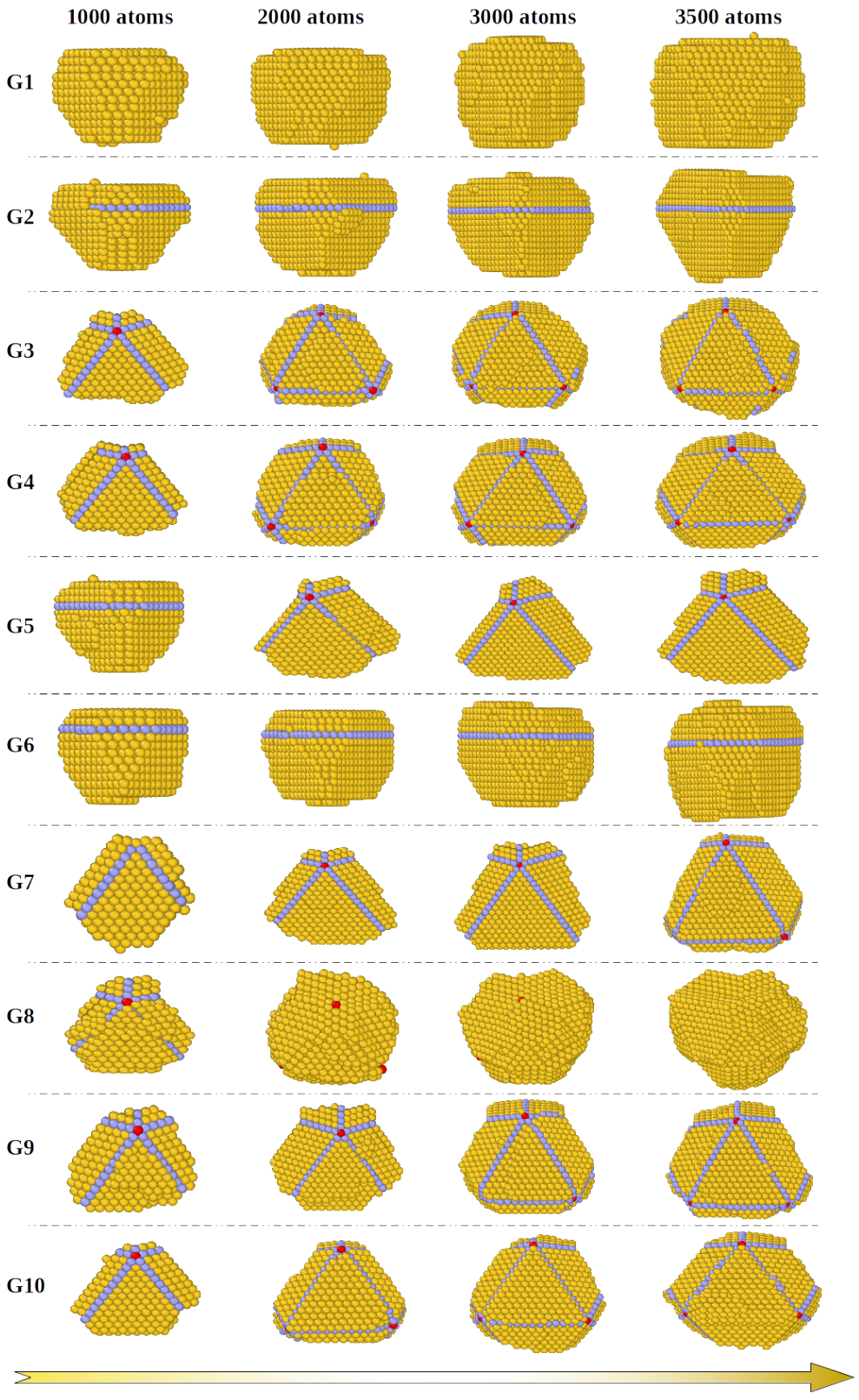

Figure S 7: Growth sequence of 10 simulations at temperature 500 K and deposition rate of 10 atoms/ns. For each simulation, four intermediate structures is shown 1000, 2000, 3000 and 3500 atoms. Five simulations goes from truncated Dh towards Ih fragments.

In Table S3 the evolution of the simulations of Figures S6 and S7 is summarized by classifying nanoparticle structures according to the number of fivefold axes they present. Structures with no fivefold axes are either double tetrahedra or disordered. Structures with one fivefold axis are growing as decahedra, whereas structures with more than one fivefold axis are evolving as icosahedral fragments.

r_{dep}	N	0 5-axes	1 5-axis	>1 5-axes
1 at/ns	1000	4	6	0
	2000	3	4	3
	3000	2	5	3
	3500	2	4	4
10 at/ns	1000	5	5	0
	2000	4	3	3
	3000	4	2	4
	3500	4	1	5

Table S 3: The structures of Figures S6 and S7 are counted according to how many fivefold axes they present.

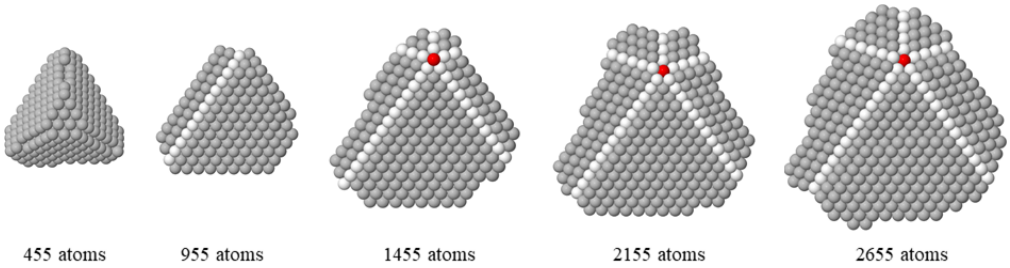

Figure S 8: Snapshots of a simulation of the growth of Ag at $T = 500$ K and deposition rate of 1 atom/ns. The simulation starts from a tetrahedral silver seed of 455 atoms.

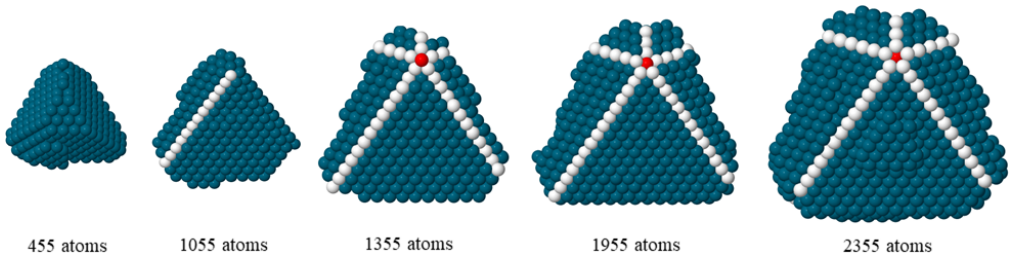

Figure S 9: Snapshots of a simulation of the growth of Pd at $T = 500$ K and deposition rate of 1 atom/ns. The simulation starts from a tetrahedral palladium seed of 455 atoms.

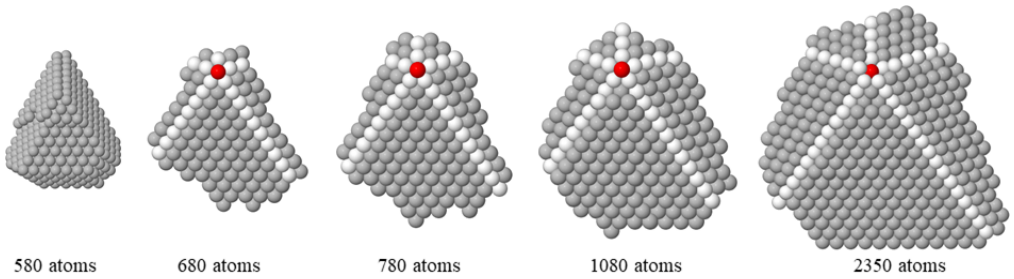

Figure S 10: Snapshots of a simulation of the growth of Ag at $T = 300$ K and deposition rate of 0.1 atom/ns. The simulation starts from a truncated tetrahedral silver seed of 580 atoms.

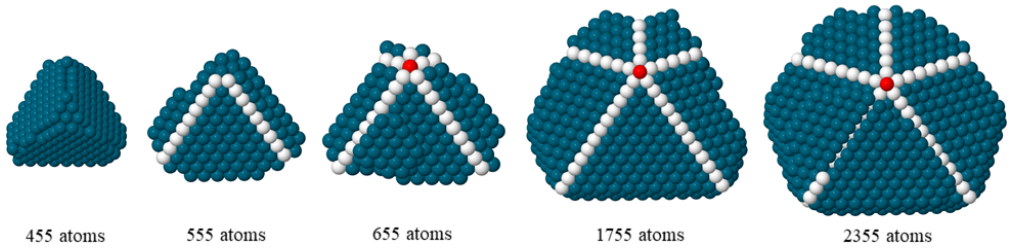

Figure S 11: Snapshots of a simulation of the growth of Pd at $T = 600$ K and deposition rate of 1 atom/ns. The simulation starts from a tetrahedral palladium seed of 455 atoms.

References

[1] F. Baletto et al. "Crossover among structural motifs in transition and noble-metal clusters". In: *J. Chem. Phys.* 116 (2002), p. 3856.

[2] F. Cyrot-Lackmann and F. Ducastelle. "Binding Energies of Transition-Metal Atoms Adsorbed on a Transition Metal". In: *Phys. Rev. B* 4 (1971), pp. 2406–2412.

[3] P. Giannozzi et al. "QUANTUM ESPRESSO: a modular and open-source software project for quantum simulations of materials". In: *J. Phys. Condens. Matter* 21 (2009), p. 395502.

[4] R. P. Gupta. "Lattice relaxation at a metal surface". In: *Phys. Rev. B* 23 (1981), p. 6265.

[5] Diana Nelli and Riccardo Ferrando. "Core-shell vs. multi-shell formation in nanoalloy evolution from disordered configurations". In: *Nanoscale* 11 (27 2019), pp. 13040–13050.

[6] Diana Nelli et al. "One-Step Growth of Core–Shell (PtPd)@Pt and (PtPd)@Pd Nanoparticles in the Gas Phase". In: *The Journal of Physical Chemistry C* 124.26 (2020), pp. 14338–14349.

[7] R.G. Parr and W. Yang. *Density-Functional Theory of Atoms and Molecules*. Oxford University Press, 1994.

[8] John Perdew, Kieron Burke, and Matthias Ernzerhof. "Generalized Gradient Approximation Made Simple". In: *Phys. Rev. Lett.* 77 (1997), pp. 3865–3868.

[9] John P. Perdew et al. "Restoring the Density-Gradient Expansion for Exchange in Solids and Surfaces". In: *Phys. Rev. Lett.* 100 (13 2008), p. 136406.

[10] V. Rosato, M. Guillopé, and B. Legrand. "Thermodynamical and structural properties of f.c.c. transition metals using a simple tight-binding model". In: *Phil. Mag. A* 59 (1989), p. 321.

[11] Dawn M. Wells et al. "Metastability of the atomic structures of size-selected gold nanoparticles". In: *Nanoscale* 7 (2015), pp. 6498–6504.

[12] Yu Xia et al. "Shape control of size-selected naked platinum nanocrystals". In: *Nat. Commun* 12 (2021), p. 3019.